Establishment and characterisation of oviductal organoids from farm and companion animals

Edwina F. Lawson[1*], Arnab Ghosh[2,3,4], Victoria Blanch[2,3,4], Christopher G. Grupen[5], R John Aitken[1], Rebecca Lim[3,4], Hannah R. Drury[3,4], Mark A. Baker[1,4], Zamira Gibb[1], Pradeep S. Tanwar[2,3,4*]

[1]Priority Research Centre for Reproductive Science; [2]Global Centre for Gynaecological Diseases; [3]School of Biomedical Sciences and Pharmacy, University of Newcastle, NSW, Australia.

[4]Hunter Medical Research Institute, New Lambton Heights, NSW, Australia

[5]Sydney School of Veterinary Science, Faculty of Science, University of Sydney, Camden, NSW, Australia.

Address correspondence to:

Dr Edwina Lawson

LS4.45, University Drive, University of Newcastle

Callaghan NSW 2308 Australia

Email: edwina.lawson@uon.edu.au

Phone: +61 2 4921 5637

Professor Pradeep S. Tanwar
Director, Global Centre for Gynecological Diseases
NHMRC R. D. Wright Career Development Fellow
LS236, University Drive, University of Newcastle
Callaghan NSW 2308 Australia
Email: pradeep.tanwar@newcastle.edu.au
Phone: +61-2-49215148

Running title: Oviductal organoids in domestic species.

Summary sentence: Organoids can be derived from the oviductal epithelium of cow, cat, dog, horse, and pig to advance assisted reproductive technologies in animals.

Key words: Oviduct, Organoids, Fertility, Disease modelling, Equine

Funding: This work is supported by the Australian Research Council (Grant number LP160100824, ZG) and NHMRC Career Development Fellowship (1159094, PT).

Declaration of interest: There is no conflict of interest that could be perceived as prejudicing the impartiality of this research.

1

ABSTRACT

Organoid technology has provided us with a unique opportunity to study early human development and decipher various steps involved in the pathogenesis of human diseases. The technology is already used in clinics to improve human patient outcomes. However, limited knowledge of the methodologies required to establish organoid culture systems in domestic animals has slowed the advancement and application of organoid technology in veterinary medicine. Here, we have developed a platform to grow organoids from animal tissue samples and characterized oviductal organoids from five domestic animal species. Organoids were grown progressively from single cells derived from the enzymatic digestion of freshly collected equine, bovine, feline, canine, and porcine oviducts. The addition of WNT, TGFB, BMP, Rock, and Notch signalling pathway activators or inhibitors in the culture medium suggested remarkable conservation of the molecular signals involved in oviductal epithelial development and differentiation across species. The gross morphology of organoids from all the domestic species was initially similar. However, some differences in size, complexity, and growth rate were observed and described. Well-defined and synchronised motile ciliated cells were observed in differentiated organoids in mature populations. Histopathologically, oviductal organoids mimicked their respective native tissue. In summary, we have developed a detailed cross-species comparison of oviductal organoid models, which will be valuable for advancing assisted reproductive technologies and fertility studies in these animal species in the future.

22 INTRODUCTION

23 The oviduct is not solely a conduit connecting the ovary to the uterus, but a complex
24 hormonally regulated organ, which is essential to sustain fertilisation and early embryonic life
25 (Lyons et al., 2006). The oviduct, known as the fallopian tube in humans, consists of four
26 functionally unique segments. Most proximal to the ovary are the fimbrial branches of the
27 infundibulum, which pick up and propel the newly ovulated oocyte to the ampulla. The ampullary
28 region is where spermatozoa undergo the final stages of capacitation and achieve fertilisation of
29 the oocyte. This region is connected to the isthmus, which is believed to play roles in both the
30 storage of spermatozoa prior to ovulation and the regulated transport of cleaving embryos. Lastly
31 is the proximately located utero-tubal junction, (Talbot et al., 1999), which is simultaneously a
32 major barrier for sperm transport (Suarez and Pacey, 2006), and the final region embryos await
33 before reaching the uterine lumen (Avilés et al., 2015). The lumen of the mammalian oviduct is
34 lined by intricately folded pseudostratified epithelial cells, containing interspersed secretory and
35 ciliated cells (Ito et al., 2020). Ciliated cells propel the oocyte by creating luminal currents through
36 continual synchronised beating of their cilia axoneme (Ezzati et al., 2014), whereas the secretory
37 cells produce the complex oviductal fluid, which provides the optimal micro-environment for
38 sperm capacitation, fertilisation and early embryonic survival (Abe and Oikawa, 1993, Chen et al.,
39 2013).

40 Like many epithelia, the oviduct contains a population of stem cell-like progenitors, which
41 actively divide to facilitate epithelial regeneration and homeostasis. Oviductal fimbriae epithelial
42 cells are regularly exposed to follicular fluid during each ovulation (Huang et al., 2015). The
43 follicular fluid contains copious inflammatory cytokines and reactive oxygen species (ROS) which
44 readily lead to tissue injury and DNA strand breakage in the cells of this region (Hamdan et al.,
45 2016, Al-Saleh et al., 2021). Thus, the oviductal fimbria epithelium is one of the tissues with most
46 abundant stemness activity, meaning it is required to maintain a balance between quiescence,

47 proliferation, and regeneration. As such, in the epithelium, secretory cells are the most frequently
48 dividing cells, which not only self-renew, but also give rise to ciliated cells. Lineage tracing work
49 has identified that such stem-cells express the secretory marker PAX8 (Ghosh et al., 2017), which
50 differentiate into ciliated cells (acetylated a-tubulin positive) through the WNT-signalling pathway
51 and play a crucial role in oviduct development and homeostasis (Kessler et al., 2015). Furthermore,
52 most proliferating cells in the oviductal epithelium are secretory cells (Ghosh et al., 2017), which
53 in humans and the mouse may be driven to differentiate into fallopian/oviductal organoids when
54 supplemented with niche factors (Kessler et al., 2015, Xie et al., 2018), further supporting their role
55 as stem/progenitor cells. Single cell sequencing analyses of human fallopian tube epithelial cells
56 have identified several different populations of these secretory cells and further studies are
57 required to clarify their contributions to oviductal epithelial homeostasis (Ahmed and Tait, 2020,
58 Dinh et al., 2021).

59 Recent advances in assisted reproductive technology (ART) have helped us to better
60 understand the causes of infertility. Even though there have been great developments in ART and
61 the importance of the oviduct for optimal gamete maturation, capacitation, and embryo
62 development has been established (Avilés et al., 2010), many unanswered biophysical questions
63 remain for domestic species. For example, in the equine, the biochemical signal for maternal
64 recognition of pregnancy (MRP) has not yet been identified (Swegen, 2021) and an efficient *in*
65 *vitro* fertilisation (IVF) protocol has not yet been established (Leemans et al., 2016). In cattle, IVF
66 is widely used in commercial settings but *in vitro* conditions for fertilisation and embryo production
67 are still far from optimal. As such, it is believed that up to 50% of pregnancy failures in dairy cattle
68 take place in the oviduct (Walsh et al., 2011). Furthermore, polyspermy is a frequent phenomenon
69 during IVF in many species, including porcine, while in an *in vivo* setting it is rarely observed
70 (Lawson et al., 2022). For companion species, such as the canine and feline, IVF is not well
71 established, and a detailed understanding of reproductive idiosyncrasies has predominantly been

72 established for the purpose of application to endangered species of non-domestic taxon
73 (Thongphakdee et al., 2020). These gaps led to the hypothesis that a species-specific oviductal
74 organoid model could be uniquely developed, and characterised for individual species. Oviductal
75 studies have the potential to advance IVF in domestic species by allowing detailed *in-vitro* studies
76 to be carried out on the microenvironment in which fertilisation and early embryo development
77 occur. Domestic animal research has the potential to improve food security and welfare outcomes,
78 while providing models for human health research (Seeger, 2020). This latter contribution is
79 recognised by the One Heath Initiative, in which the close linkage between the health of humans,
80 animals and the environment is widely accepted (Seeger, 2020). As such, organoids will be
81 valuable for evaluating cross-species disease variations or species-specific infectivity of zoonotic
82 pathogens, while providing an *in vitro* alternative for infection studies (Kawasaki et al., 2022).
83 In a clinical setting, organoids may be cultured from specific patients to conduct *in vitro*
84 drug efficacy testing for tailored treatments (Berkers et al., 2019), facilitating personalised
85 medicine into clinical practice. Oviductal organoids composed of fully differentiated ciliated and
86 secretory epithelial cells have been successfully generated from human (Kessler et al., 2015, Chang
87 et al., 2020) and mouse-derived cells (Xie et al., 2018, Ghosh et al., 2020). While these systems
88 have vastly improved the understanding of pathologies and the process of fertilisation in each of
89 these species, their applicability to other animals is limited because oviductal physiology and
90 fertilisation strategies vary greatly between mammalian species. As such, the aim of this study was
91 to carry out a detailed cross-species comparison of oviductal organoid development, with the
92 intention to provide advancements for both ART and studies of fertility.
93

MATERIAL AND METHODS

Oviduct epithelium isolation and organoid culture

Whole oviducts were obtained from adult porcine (n=3), bovine (n=2), equine (n=4), canine (n=5) and feline (n=4) females, and samples were collected either directly from the slaughterhouse or abattoir floor or collected from discarded post-surgical hysterectomy material. As this work was conducted using opportunistic sourcing of discarded tissues and organs, no formal institutional animal ethics committee approval was required. After collection, samples were then washed and transported on ice in a transportation medium (Dulbecco's Modified Eagle Medium/Nutrient Mixture F-12 (DMEM-F12 cat # 12634-010) with 1% penicillin-streptomycin (Life Technologies, cat # 15070-063)) and stored in at 4°C overnight in the same medium. Oviducts were washed three times with Dulbecco's phosphate-buffered saline (DPBS) and 1% penicillin-streptomycin to remove the blood and unwanted debris. Multiple small portions of the fimbriae were dissected under a stereomicroscope and digested in Accumax (Innovative Cell Technologies, Inc., cat#AM105) enzyme for 2-3 hours on a shaker at room temperature. Enzymatic digestion was stopped by adding a complete medium comprising 5% foetal bovine serum (FBS), 1% Glutamax (Sigma), 1% HEPES and 1% penicillin-streptomycin in Advanced DMEM-F12. The cell suspension was collected in a Falcon tube and centrifuged at 1500 rpm for 5 minutes to collect the epithelial cells. These epithelial cells were then propagated in a complete medium supplemented with the addition of human Epidermal Growth Factor (hEGF) (12ng/ml, PeproTech), ROCK inhibitor (Y-27632; 10 mM; TOCRIS) and Primocin (0.2%) as a 2-dimensional culture on a matrigel coated cell culture plate. Once 70% confluence had been achieved, epithelial cells were detached by trypsinisation and centrifuged at 1500 rpm for 5 min to collect the epithelial cells. Epithelial cells in a fresh complete medium were then incubated for 2.5-3 h at 37°C, in a 5% CO2 incubator for differential attachment to enrich pure epithelial cells. After epithelial cell enrichment, the cells were counted and resuspended in a complete medium without FBS, referred to as Oviductal Epithelial (OE) culture

119 medium. Following this, the epithelial cells were mixed with matrigel and placed as a 50 µl drop
120 in each well of a 24-well cell culture plate, with 25,000 cells in each 50 ul drop. The matrigel with
121 cells was allowed to solidify by keeping the 24-well plate at 37°C for 20 minutes. Then each well
122 of the culture plate was overlaid with 75% OE medium and 25% WNT3A-RSPO3-NOGGIN
123 conditioned medium (WRN-CM) prepared from L-WRN cells by following a previously described
124 protocol (Miyoshi et al., 2013).
125 The medium was further supplemented with growth factors and signalling modulators comprising
126 of human Epidermal Growth Factor (hEGF) (12ng/ml, PeproTech), B27 Supplement (2%, Gibco),
127 ROCK inhibitor (Y-27632 dihydrochloride; 5 mM; TOCRIS), N-Acetyl-L-Cysteine (1.25 mM/ml,
128 Sigma), Nicotinamide (10 mM/ml, Sigma), Primocin (0.2%, Invivogen), and A83-01 (0.5 mM,
129 TOCRIS). The medium for organoid culture was replenished every three days and on day 21 the
130 organoids were harvested for further processing. For each sample, 25-30 organoids were
131 considered at each time point for each species.

132 Immunofluorescence (IF) and Hematoxylin & Eosin (H&E)

133 Oviductal tissues were fixed in 4% (w/v) paraformaldehyde at 4°C overnight before being
134 processed for paraffin embedding. Organoids were fixed in 4% (w/v) paraformaldehyde for one
135 hour at room temperature. The paraffin-embedded blocks were then sectioned at 5 µm thickness.
136 For IF and H&E staining, 5 µm sections were deparaffinised followed by rehydration, and
137 processed separately according to protocol. For immunofluorescence staining, antigen retrieval
138 was carried out on rehydrated sections by heating them to either at 110°C (oviductal tissue) or
139 98°C (organoids) for 30 minutes in EDTA buffer (1mM; pH 8.0). After blocking, sections were
140 incubated with primary antibodies at 4°C overnight. The primary antibodies used were rabbit anti-
141 PAX8 (1:1000; catalog number 10336-1-AP; Proteintech), mouse anti-Acetylated-Tubulin (1:1000;
142 catalog number T7451, clone 6-11B-1, Sigma-Aldrich), rabbit anti-Ki67 (1:400; catalog number

143 Ab15580, Abcam) and DAPI dilactate (Sigma-Aldrich D9564). The secondary antibodies were
144 Alexa 488/594 conjugated anti-rabbit/mouse IgG (1:250; Jackson ImmunoResearch Labs).

145 Microscopy and image acquisition

146 Initial gross oviductal images were captured using Nikon SMZ25 stereoscope. During
147 organoid culture, organoid development images were taken by JuLiTM Stage Real-Time Cell
148 History Recorder (NanoEnTek) every 3 days. Fluorescence and H&E images were acquired using
149 Olympus DP80 CCD (charge-coupled device) and cellSens software (Olympus). Confocal laser
150 scanning was carried out on a Zeiss LSM 900-Airyscan-2 microscope with a 63x objective using the
151 software ZEN (blue edition) 3.0 and were reconstructed by sequences (z-stack), organoid imaging
152 measurement and analysis software was carried out using Fiji 9 (ImageJ) (Schindelin et al., 2012).

153 Mature organoids containing cilia were transferred to a recording chamber at room
154 temperature (22–25 °C), containing OE culture medium and perfused at a rate of two bath volumes
155 per minute (i.e. 3 ml/min), Cilia was observed under a Zeiss Axioskop microscope using infra-red
156 differential interference contrast optics and a Zeiss AxioCam Mrm camera. From the equine and
157 porcine organoid populations, cilia were identified and imaged using Zen Blue software (version
158 2.6) and live ciliary motions were recorded from 12 regions of ciliated axonemes at 30 second
159 intervals. The recording captured a synchronous and continual beating of motile cilia which
160 generated a coordinated and unidirectional flow in both species (Supp. 1).

161

162 RESULTS

163 Gross and histological characterization of oviducts from domestic animals

164 Healthy feline, canine, porcine, bovine, and equine oviducts were collected, and gross
165 images of morphological infundibular characteristics of each species were obtained, as shown
166 (Figure 1i). Despite the infundibulum serving the same function across the species, namely, to
167 collect ovulated oocytes and transport them, clear morphological differences were evident.
168 Macroscopically, the infundibulum presents with funnel-shaped irregular projections (white arrows)
169 with branching fimbriae engulfing the ovary. Interestingly, cat and dog infundibulum adhere tightly
170 to the ovary (Fig1i A, Fig1i B). In the case of the porcine, equine, and canine, the fimbriae fonds
171 branch more loosely around the ovary without being attached (Fig1i C, Fig1i D, Fig1i E,). Oviductal
172 sectioning, followed by H&E staining (Figure 1ii) showed the histological architecture of native
173 oviducts, including all three distinct layers, serosa, muscularis and mucosa. The oviductal
174 epithelium from each species comprised a single convoluted layer of columnar epithelial cells
175 lining the lumen, creating both luminal projections and differently shaped crypts.

176 Distribution of secretory and ciliated cells in oviducts

177 Immunofluorescence (IF) analysis of native oviductal epithelium showed a consistent
178 expression of PAX8-positive secretory epithelial cells located mostly along the basal region with a
179 cohesive apical-to-basal polarity (Image 1iii). Using DAPI as a nuclear counterstain, acetylated α-
180 tubulin (Ac-Tub) was used to identify the flagella-like projections of the ciliated cells by staining
181 the acetylated microtubules found within centrioles and cilia. Notably, in the cat and dog, Ac-Tub
182 positive ciliated cells were consistently expressed but punctate and more irregularly spaced
183 throughout the infundibulum (Fig1iii A, Fig1iii B), compared to porcine, bovine, and equine
184 oviducts (Fig1iii C, Fig1iii D, Fig1iii E). Additionally, Ki67, the nuclear DNA-binding protein strictly
185 associated with cell proliferation, was constitutively dispersed throughout normal healthy oviductal

186 epithelium (Fig 1iv). The presence of Ki67 and its distribution suggests that cells are actively
187 dividing.

188 Establishment of oviductal organoids cultures

189 The fimbrial end of equine, porcine, bovine, canine, and feline oviducts were collected.
190 Single cells were isolated using enzymatic digestion. These single cells were embedded in matrigel
191 and supplemented in the culture medium with required growth and niche factors. Organoids
192 progressively developed from single cells over the course of 21days. The organoids were imaged
193 every 3 days (Fig. 2), to record a timeline of the visual change occurring in the cultures, which
194 included recording morphological changes and size, as measured by perimeter (μm). During the
195 initial phase of growth, no ciliated cells or ciliary beating were observed, however, these cells
196 appeared after 10 days of cultures. Cultures were efficiently generated long-term and maintained
197 for several months. Organoids were also successfully grown from cells frozen in liquid nitrogen.

198 Species variation in organoid phenotype and growth

199 For each species, cultured organoid growth was consistent, but between species, organoid
200 expansion and size progressed along different trajectories. From day 6, a marked expansion in
201 size was observed for each species (Fig2ii). However, feline oviductal organoids had exponential
202 growth in size (perimeter) from day 6 (Fig2ii.A), showing a notably higher rate of expansion from
203 that point compared to other species (Fig2ii B,C,D,E). Collectively, maximal organoid size growth
204 occurred between day 12 and day 18 (Fig2iii). In addition to sharing prominent morphological
205 characteristics, such as ciliation, phenotypic differences were immediately apparent between the
206 species. Evident after day 18, equine and bovine organoids lost the spheroid phenotype (Fig2iv.D,
207 E), and by day 21 more complex cell configurations developed. Organoids from all species
208 developed crypts and villi-like structures and internal folding architecture and invaginations, which
209 were analogous to the mucosal structure of the native oviduct (Fig2v.D, E). The branching
210 architecture was particularly and consistently evident in the equine, as highlighted by comparing

211 the morphological differences of mature feline (Fig 3A) and equine oviductal organoids (Fig 3B).
212 To determine if the organoid cell-network architecture was similar to that observed in the native
213 oviductal epithelium (Fig 4), H&E staining was carried out on oviductal organoid full-thickness
214 sections (Fig 4i) after 21 days of culture. Staining showed that oviductal organoids were composed
215 of a monolayer of polarised columnar epithelial cells, exhibiting equivalent complex internal
216 folding architectural structures.

217 Immunostaining of organoid cultures

218 For further comparison, individual cultures were stained with PAX8, Ac-Tub and Ki67, with
219 DAPI serving as a nuclear counterstain after 21 days of culture (Fig 4ii). Mature organoids
220 consistently expressed PAX8-positive secretory cells as well as PAX8-negative Ac-Tub-positive
221 ciliated cells (Fig 4iii). Given that the highly proliferating PAX8 cells respond to clear Wnt
222 signalling, which modulates differentiation into ciliated cells (Stewart and Behringer, 2012), their
223 presence in oviductal organoids is indicative of epithelial cell homeostasis. Interspersed Ki67-
224 positive proliferating cells were detected scattered at the basal layer of the epithelium (Fig 4iii),
225 demonstrating active proliferation in each population. Interestingly, the IF revealed that much of
226 the expression patterns in oviductal organoids, such as the proliferation patterns of Ki67 positive
227 cells, and the consistency of PAX8, Ac-Tub positive cells, consistently mimicked native oviductal
228 epithelium.

229 Functional analysis of cilia

230 Acetylated alpha-tubulin-positive cilia were identified, projecting luminally in mature
231 organoids of all species. Moreover, across all species, and consistent with native oviductal
232 epithelium. The presence and detail of Ac-Tub-positive cells with visible cilia were captured with
233 high magnification using IF confocal imaging (Fig 5), such ciliated cells contained abundant well-
234 defined cilia that were apically pointed and anchored to well-aligned basal bodies. For functional
235 validation of the model, mature organoids should possess a functional ciliary axoneme capable of

236 generating a unidirectional flow and a ciliary beat. As such, motile cilia were observed consistently
237 in the mature organoid population, with mature cilia vigorously motile and recorded using high-
238 speed infra-red differential interference contrast optics. A synchronised, continual beat was
239 recorded in both equine and porcine with actively motile cilia generating a coordinated and
240 continual, unidirectional flow (Supp. 1), of secretion, debris, and medium.

241 Quantification of organoid development

242 For quantification of organoid development, individual organoids (n=25) were measured
243 from each sample, for each species, and the mean area (μm^2) recorded, at 1, 6, 12, 18 and 21 days
244 of culture (Fig6a). To quantify the distinct changes in morphology, the principles of morphometrics
245 were applied using perimeter to area ratio to measure structural complexity (Gardiner et al., 2018,
246 Posamentier and Lehmann, 2011). Canine, porcine, bovine, and equine organoids displayed a
247 high measure of biological structure complexity (Fig6.B), particularly when compared to the rapidly
248 enlarging perimeter observed in the mature feline organoids. Importantly, the oviductal organoid
249 populations developed from single cells and progressively grew in size. For each species, this size
250 was compared, using area (μm2) growth per day (Fig6C) and the distribution of organoid sizes
251 over 21 days of culture was recorded (Fig6D).

252

253 DISCUSSION

254 The purpose of this study was to develop and characterise adult stem cell-derived oviductal
255 organoid cultures across multiple domestic species. By developing a standardised model, this
256 study found that the mature oviductal organoids that were produced resembled their source
257 tissues architecturally, structurally, and functionally. In this study, a standardised model was
258 successfully generated. Initially, internal architecture was shown to develop in individual
259 organoids, and mimic the internal architecture of native organoidal epithelia. Such architecture
260 was highlighted using H&E staining and reflected native oviductal tissue (Fig 1). It has previously
261 been shown that within oviductal epithelia, the secretory cells continuously replenish, by
262 transitioning to ciliated cells (Ghosh et al., 2017). In the present study, the progenitor secretory
263 cell marker PAX8 was consistently present in mature oviductal organoids in all species investigated
264 (Fig 4i). The presence of such progenitor cells suggests that oviductal regeneration and
265 homeostasis is occurring in the organoid populations. Furthermore, Ki67, a marker of proliferation,
266 was also observed in organoid populations, indicating that they were actively dividing (Fig 4ii).
267 The identification of Ki67 and PAX8 in these organoids is an important finding, but even more
268 notable was the presence of mature, functionally motile ciliated axonemes in organoid populations
269 in 21 day organoids. Cells containing mature ciliated axonemes were initially identified by the
270 presence of Ac-Tub (Fig 5), and detailed images of these structures were captured. In addition,
271 these cilia were observed to produce a synchronous and continual beat frequency resulting in a
272 unidirectional flow (Supp 1). As the mammalian oviduct is one of the organs that relies heavily on
273 the motility of cilia for its normal functions (Wang et al., 2015), the identification of actively motile
274 cilia supports the functionality of the organoid model described in this manuscript.

275 Anatomically, the proportion of ciliated cells is most numerous in the distal oviduct (fimbria,
276 infundibulum and ampulla) (Stewart and Behringer, 2012). Previous studies have shown that stem-
277 like cells are found in the fimbrial region of the oviduct in the mouse and human (Das et al., 2006,

278 Yamamoto et al., 2016, Paik et al., 2012, Patterson and Pru, 2013), and include PAX8 progenitors
279 cells, that transition, giving rise to ciliated cells (Ghosh et al., 2017). Given that fimbrial cells
280 possess the highest organoid-forming capacity (Xie et al., 2018, Rose et al., 2020), it was this
281 anatomical region which was harvested for this study. However, the collection of such oviductal
282 specimens, was limited to those discarded samples, as such, the cyclicity, precise age and exact
283 health status could not always be accounted for in the present study. Yet, the findings seem to
284 provide a framework for models in species other than human or mouse (Rose et al., 2020, Kessler
285 et al., 2015).

286 Although mature organoids were observed in all species by 21 days, the interspecies
287 differences in oviductal development rate and structure was not surprising. Many mammalian
288 species display unique features in fertilisation physiology and early embryo development. For
289 example, in the bitch, the oocyte is released two or three days prior to fertilisation (Avilés et al.,
290 2015), rather than at the time of ovulation. In the mare, the developing embryo remains in the
291 oviduct for 5 days after fertilisation (Betteridge et al., 1982, Freeman et al., 1991), contrasting
292 markedly with the cow and sow, in which the embryo/s remain in the oviduct for only 3 and 2 days
293 respectively (Hafez and Hafez, 2016, Dziuk, 1985). In addition, parity size should be taken into
294 account when considering the function of the oviduct; the sow can carry 16 piglets per gestation,
295 whereas in the mare, similar to the human female, only one offspring is typically carried to term.
296 Such functional idiosyncrasies must be considered when comparing oviductal epithelium. In this
297 study, the comparative differences in organoid size (seen in the feline) and complexity observed
298 (in the equine) may indeed relate to the different patterns of early embryonic development
299 between species. The different growth trajectories and proliferation rates of the organoids at
300 different time points during *in vitro* culture may reflect the species-specific differences in oviductal
301 tube physiology (Avilés et al., 2010). Given that reproductive science, plays a critical role in human
302 health, it is remarkable that approximately only 10% of mammals have been studied in this field

303 (Wildt et al., 2010). Knowledge gained from such cross-species comparisons highlights the
304 diversity that exists (Nagashima and Songsasen, 2021), and how the lack of species-specific
305 studies in reproductive physiology contributes to reduced fertility rates. In a commercial setting,
306 poor fertility often translates to financial losses for producers and compromised welfare arising
307 from repeated invasive veterinary interventions (Li and Winuthayanon, 2017). So, although IVF
308 techniques have progressed over the last 40 years, and are now used in multiple domestic and
309 non-domestic species around the world (Sirard, 2018), they are not completely matured; and a
310 number of problems remain unsolved or not yet optimised (Ferré et al., 2020). IVF in the bovine
311 species is of particular interest, with its commercial scale now comparable to human IVF (Sirard,
312 2018). Likewise, for the equine, however intra-cytoplasmic sperm injection (ICSI) is currently the
313 only commercial method for producing equine embryos *in vitro*. Research in the equine has
314 recently focused on the early secretions of both the embryo and the maternal host (Swegen et al.,
315 2017, Lawson et al., 2018, Smits et al., 2018, Fernández-Hernández et al., 2021) and highlighted
316 the need for a more profound study of the oviduct. As species-specific differences between
317 mammals are notable and varied, the traditional medical-model; beginning on laboratory rodents
318 before clinical translation to humans (Bourdon et al., 2021) or mammal; is less than ideal. On these
319 grounds, individualised organoid models derived from farm and companion animals have great
320 potential to contribute to veterinary medicine as well as the health of the human population. The
321 insights gained may benefit human fertility treatments and wildlife conservation efforts.

322 This study has succeeded in defining and characterising the growth and differentiation of
323 oviductal organoids in domestic species and, in so doing, has demonstrated the effectiveness of
324 a methodology that can be applied to future research on the reproductive biology of key livestock
325 species. The development of an oviductal organoid model for domestic animal species allows
326 direct access to the environment in which conception and early embryonic development occurs.
327 As such it creates a platform for investigating the key attributes of a biologically supportive

oviductal environment, which may include, but is not limited to further investigations into oviductal secretion, oviductal biomechanics, and the influence of the oviductal milieu on both embryo and spermatozoa. Such models will play a crucial role in addressing key issues relating to the efficacy of ART procedures, advances in animal welfare and the preservation of diversity. Furthermore, given that the oviduct is the site of sperm capacitation, fertilisation and early embryonic life, the findings of this study open up the potential to use this organoid model to achieve fundamental insights into the understanding of processes that are critical for the reproductive process both *in vivo* and *in vitro.*

Author contribution

E.L., Z.G., R.J.A., P.T. Designed research; E.L., A.G., V.B., H.D. Performed research; H.D., R.L., M.B. Contributed new reagents; E.L., A.G., V.B., H.D. Analyzed data; E.L., M.B., Z.G., R.J.A., P.T. Wrote the paper.

Acknowledgements

We would like to thanks members of the PRC for Reproduction, and the Australian Research Council, for supporting this work.

346 REFERENCES

347 ABE, H. & OIKAWA, T. 1993. Observations by scanning electron microscopy of oviductal epithelial
348 cells from cows at follicular and luteal phases. *The Anatomical Record,* 235**,** 399-410.
349 AHMED, A. & TAIT, S. W. G. 2020. Targeting immunogenic cell death in cancer. *Molecular*
350 *Oncology,* 14**,** 2994-3006.
351 AL-SALEH, I., COSKUN, S., AL-ROUQI, R., AL-RAJUDI, T., ELTABACHE, C., ABDULJABBAR, M. &
352 AL-HASSAN, S. 2021. Oxidative stress and DNA damage status in couples undergoing in
353 vitro fertilization treatment. *Reprod Fertil,* 2**,** 117-139.
354 AVILÉS, M., COY, P. & RIZOS, D. 2015. The oviduct: A key organ for the success of early
355 reproductive events. *Animal Frontiers,* 5**,** 25-31.
356 AVILÉS, M., GUTIÉRREZ-ADÁN, A. & COY, P. 2010. Oviductal secretions: will they be key factors
357 for the future ARTs? *Molecular Human Reproduction,* 16**,** 896-906.
358 BERKERS, G., VAN MOURIK, P., VONK, A. M., KRUISSELBRINK, E., DEKKERS, J. F., DE WINTER-
359 DE GROOT, K. M., ARETS, H. G. M., MARCK-VAN DER WILT, R. E. P., DIJKEMA, J. S.,
360 VANDERSCHUREN, M. M., HOUWEN, R. H. J., HEIJERMAN, H. G. M., VAN DE GRAAF,
361 E. A., ELIAS, S. G., MAJOOR, C. J., KOPPELMAN, G. H., ROUKEMA, J., BAKKER, M.,
362 JANSSENS, H. M., VAN DER MEER, R., VRIES, R. G. J., CLEVERS, H. C., DE JONGE, H. R.,
363 BEEKMAN, J. M. & VAN DER ENT, C. K. 2019. Rectal Organoids Enable Personalized
364 Treatment of Cystic Fibrosis. *Cell Reports,* 26**,** 1701-1708.e3.
365 BETTERIDGE, K. J., EAGLESOME, M. D., MITCHELL, D., FLOOD, P. F. & BERIAULT, R. 1982.
366 Development of horse embryos up to twenty two days after ovulation: observations on
367 fresh specimens. *J Anat,* 135**,** 191-209.
368 BOURDON, G., CADORET, V., CHARPIGNY, G., COUTURIER-TARRADE, A., DALBIES-TRAN, R.,
369 FLORES, M.-J., FROMENT, P., RALIOU, M., REYNAUD, K., SAINT-DIZIER, M. & JOUNEAU,
370 A. 2021. Progress and challenges in developing organoids in farm animal species for the
371 study of reproduction and their applications to reproductive biotechnologies. *Veterinary*
372 *research,* 52**,** 42-42.
373 CHANG, Y.-H., CHU, T.-Y. & DING, D.-C. 2020. Human fallopian tube epithelial cells exhibit
374 stemness features, self-renewal capacity, and Wnt-related organoid formation. *Journal of*
375 *Biomedical Science,* 27**,** 32.
376 CHEN, S., EINSPANIER, R. & SCHOEN, J. 2013. In vitro mimicking of estrous cycle stages in
377 porcine oviduct epithelium cells: estradiol and progesterone regulate differentiation, gene
378 expression, and cellular function. *Biology of reproduction,* 89**,** 54, 1-12.
379 DAS, S., CHATTOPADHYAY, R., GHOSH, S., GHOSH, S., GOSWAMI, S. K., CHAKRAVARTY, B. N.
380 & CHAUDHURY, K. 2006. Reactive oxygen species level in follicular fluid—embryo quality
381 marker in IVF? *Human Reproduction,* 21**,** 2403-2407.
382 DINH, H. Q., LIN, X., ABBASI, F., NAMEKI, R., HARO, M., OLINGY, C. E., CHANG, H.,
383 HERNANDEZ, L., GAYTHER, S. A., WRIGHT, K. N., ASPURIA, P. J., KARLAN, B. Y.,
384 CORONA, R. I., LI, A., RIMEL, B. J., SIEDHOFF, M. T., MEDEIROS, F. & LAWRENSON, K.
385 2021. Single-cell transcriptomics identifies gene expression networks driving differentiation
386 and tumorigenesis in the human fallopian tube. *Cell Rep,* 35**,** 108978.
387 DZIUK, P. 1985. Effect of migration, distribution and spacing of pig embryos on pregnancy and
388 fetal survival. *J Reprod Fertil Suppl,* 33**,** 57-63.
389 EZZATI, M., DJAHANBAKHCH, O., ARIAN, S. & CARR, B. R. 2014. Tubal transport of gametes and
390 embryos: a review of physiology and pathophysiology. *Journal of assisted reproduction*
391 *and genetics,* 31**,** 1337-1347.
392 FERNÁNDEZ-HERNÁNDEZ, P., MARINARO, F., SÁNCHEZ-CALABUIG, M. J., GARCÍA-MARÍN, L.
393 J., BRAGADO, M. J., GONZÁLEZ-FERNÁNDEZ, L. & MACÍAS-GARCÍA, B. 2021. The

Proteome of Equine Oviductal Fluid Varies Before and After Ovulation: A Comparative Study. *Front Vet Sci,* 8**,** 694247.

FERRÉ, L. B., KJELLAND, M. E., STRØBECH, L. B., HYTTEL, P., MERMILLOD, P. & ROSS, P. J. 2020. Review: Recent advances in bovine in vitro embryo production: reproductive biotechnology history and methods. *Animal,* 14**,** 991-1004.

FREEMAN, D. A., WEBER, J. A., GEARY, R. T. & WOODS, G. L. 1991. Time of embryo transport through the mare oviduct. *Theriogenology,* 36**,** 823-830.

GARDINER, J. D., BEHNSEN, J. & BRASSEY, C. A. 2018. Alpha shapes: determining 3D shape complexity across morphologically diverse structures. *BMC evolutionary biology,* 18**,** 184-184.

GHOSH, A., SYED, S. M., KUMAR, M., CARPENTER, T. J., TEIXEIRA, J. M., HOUAIRIA, N., NEGI, S. & TANWAR, P. S. 2020. In Vivo Cell Fate Tracing Provides No Evidence for Mesenchymal to Epithelial Transition in Adult Fallopian Tube and Uterus. *Cell Rep,* 31**,** 107631.

GHOSH, A., SYED, S. M. & TANWAR, P. S. 2017. In vivo genetic cell lineage tracing reveals that oviductal secretory cells self-renew and give rise to ciliated cells. *Development,* 144**,** 3031-3041.

HAFEZ, E. S. E. & HAFEZ, B. 2016. Fertilization and Cleavage. *Reproduction in Farm Animals.* 7th ed. Philadelphia: Lippincott Williams & Wilkins.

HAMDAN, M., JONES, K. T., CHEONG, Y. & LANE, S. I. 2016. The sensitivity of the DNA damage checkpoint prevents oocyte maturation in endometriosis. *Sci Rep,* 6**,** 36994.

HUANG, H.-S., CHU, S.-C., HSU, C.-F., CHEN, P.-C., DING, D.-C., CHANG, M.-Y. & CHU, T.-Y. 2015. Mutagenic, surviving and tumorigenic effects of follicular fluid in the context of p53 loss: initiation of fimbria carcinogenesis. *Carcinogenesis,* 36**,** 1419-1428.

ITO, S., YAMAMOTO, Y. & KIMURA, K. 2020. Analysis of ciliogenesis process in the bovine oviduct based on immunohistochemical classification. *Mol Biol Rep,* 47**,** 1003-1012.

KAWASAKI, M., GOYAMA, T., TACHIBANA, Y., NAGAO, I. & AMBROSINI, Y. M. 2022. Farm and Companion Animal Organoid Models in Translational Research: A Powerful Tool to Bridge the Gap Between Mice and Humans. *Front Med Technol,* 4**,** 895379.

KESSLER, M., HOFFMANN, K., BRINKMANN, V., THIECK, O., JACKISCH, S., TOELLE, B., BERGER, H., MOLLENKOPF, H. J., MANGLER, M., SEHOULI, J., FOTOPOULOU, C. & MEYER, T. F. 2015. The Notch and Wnt pathways regulate stemness and differentiation in human fallopian tube organoids. *Nat Commun,* 6**,** 8989.

LAWSON, E. F., GIBB, Z., DE RUIJTER-VILLANI, M., SMITH, N. D., STOUT, T. A., CLUTTON-BROCK, A., AITKEN, J. R. & SWEGEN, A. 2018. Proteomic Analysis of Pregnant Mare Uterine Fluid. *Journal of Equine Veterinary Science,* 66.

LAWSON, E. F., GRUPEN, C. G., BAKER, M. A., AITKEN, R. J., SWEGEN, A., POLLARD, C.-L. & GIBB, Z. 2022. Conception and early pregnancy in the mare: lipidomics the unexplored frontier. *Reproduction and Fertility,* 3**,** R1-R18.

LEEMANS, B., GADELLA, B. M., STOUT, T. A., DE SCHAUWER, C., NELIS, H., HOOGEWIJS, M. & VAN SOOM, A. 2016. Why doesn't conventional IVF work in the horse? The equine oviduct as a microenvironment for capacitation/fertilization. *Reproduction,* 152**,** R233-r245.

LI, S. & WINUTHAYANON, W. 2017. Oviduct: roles in fertilization and early embryo development. *J Endocrinol,* 232**,** R1-R26.

NAGASHIMA, J. B. & SONGSASEN, N. 2021. Canid Reproductive Biology: Norm and Unique Aspects in Strategies and Mechanisms. *Animals : an open access journal from MDPI,* 11**,** 653.

PAIK, D. Y., JANZEN, D. M., SCHAFENACKER, A. M., VELASCO, V. S., SHUNG, M. S., CHENG, D., HUANG, J., WITTE, O. N. & MEMARZADEH, S. 2012. Stem-like epithelial cells are

442 concentrated in the distal end of the fallopian tube: a site for injury and serous cancer
443 initiation. *Stem Cells,* 30**,** 2487-97.
444 PATTERSON, A. L. & PRU, J. K. 2013. Long-term label retaining cells localize to distinct regions
445 within the female reproductive epithelium. *Cell Cycle,* 12**,** 2888-98.
446 POSAMENTIER, A. S. & LEHMANN, I. 2011. *The Glorious Golden Ratio*, Prometheus Books.
447 ROSE, I. M., BIDARIMATH, M., WEBSTER, A., GODWIN, A. K., FLESKEN-NIKITIN, A. & NIKITIN,
448 A. Y. 2020. WNT and inflammatory signaling distinguish human Fallopian tube epithelial
449 cell populations. *Scientific reports,* 10**,** 1-14.
450 SCHINDELIN, J., ARGANDA-CARRERAS, I., FRISE, E., KAYNIG, V., LONGAIR, M., PIETZSCH, T.,
451 PREIBISCH, S., RUEDEN, C., SAALFELD, S., SCHMID, B., TINEVEZ, J.-Y., WHITE, D. J.,
452 HARTENSTEIN, V., ELICEIRI, K., TOMANCAK, P. & CARDONA, A. 2012. Fiji: an open-
453 source platform for biological-image analysis. *Nature Methods,* 9**,** 676-682.
454 SEEGER, B. 2020. Farm animal-derived models of the intestinal epithelium: recent advances and
455 future applications of intestinal organoids. *Alternatives to Laboratory Animals,* 48**,** 215-233.
456 SIRARD, M.-A. 2018. 40 years of bovine IVF in the new genomic selection context. *Reproduction,*
457 156**,** R1-R7.
458 SMITS, K., WILLEMS, S., VAN STEENDAM, K., VAN DE VELDE, M., DE LANGE, V., VERVERS, C.,
459 ROELS, K., GOVAERE, J., VAN NIEUWERBURGH, F., PEELMAN, L., DEFORCE, D. & VAN
460 SOOM, A. 2018. Proteins involved in embryo-maternal interaction around the signalling of
461 maternal recognition of pregnancy in the horse. *Scientific Reports,* 8**,** 5249.
462 STEWART, C. A. & BEHRINGER, R. R. 2012. Mouse Oviduct Development. *In:* KUBIAK, J. Z. (ed.)
463 *Mouse Development: From Oocyte to Stem Cells.* Berlin, Heidelberg: Springer Berlin
464 Heidelberg.
465 SUAREZ, S. S. & PACEY, A. A. 2006. Sperm transport in the female reproductive tract. *Hum Reprod*
466 *Update,* 12**,** 23-37.
467 SWEGEN, A. 2021. Maternal recognition of pregnancy in the mare: does it exist and why do we
468 care? *Reproduction,* 161**,** R139-r155.
469 SWEGEN, A., GRUPEN, C. G., GIBB, Z., BAKER, M. A., DE RUIJTER-VILLANI, M., SMITH, N. D.,
470 STOUT, T. A. E. & AITKEN, R. J. 2017. From Peptide Masses to Pregnancy Maintenance:
471 A Comprehensive Proteomic Analysis of The Early Equine Embryo Secretome, Blastocoel
472 Fluid, and Capsule. *PROTEOMICS,* 17**,** 1600433.
473 TALBOT, P., GEISKE, C. & KNOLL, M. 1999. Oocyte pickup by the mammalian oviduct. *Molecular*
474 *biology of the cell,* 10**,** 5-8.
475 THONGPHAKDEE, A., SUKPARANGSI, W., COMIZZOLI, P. & CHATDARONG, K. 2020.
476 Reproductive biology and biotechnologies in wild felids. *Theriogenology,* 150**,** 360-373.
477 WALSH, S., WILLIAMS, E. & EVANS, A. 2011. A review of the causes of poor fertility in high milk
478 producing dairy cows. *Animal reproduction science,* 123**,** 127-138.
479 WANG, S., BURTON, J. C., BEHRINGER, R. R. & LARINA, I. V. 2015. In vivo micro-scale
480 tomography of ciliary behavior in the mammalian oviduct. *Scientific Reports,* 5**,** 13216.
481 WILDT, D. E., COMIZZOLI, P., PUKAZHENTHI, B. & SONGSASEN, N. 2010. Lessons from
482 biodiversity—the value of nontraditional species to advance reproductive science,
483 conservation, and human health. *Molecular Reproduction and Development: Incorporating*
484 *Gamete Research,* 77**,** 397-409.
485 XIE, Y., PARK, E.-S., XIANG, D. & LI, Z. 2018. Long-term organoid culture reveals enrichment of
486 organoid-forming epithelial cells in the fimbrial portion of mouse fallopian tube. *Stem Cell*
487 *Research,* 32**,** 51-60.
488 YAMAMOTO, Y., NING, G., HOWITT, B. E., MEHRA, K., WU, L., WANG, X., HONG, Y., KERN, F.,
489 WEI, T. S., ZHANG, T., NAGARAJAN, N., BASULI, D., TORTI, S., BREWER, M., CHOOLANI,
490 M., MCKEON, F., CRUM, C. P. & XIAN, W. 2016. In vitro and in vivo correlates of

491 physiological and neoplastic human Fallopian tube stem cells. *The Journal of Pathology*,
492 238, 519-530.
493

Figure 1. Characterisation of feline (A), canine (B), porcine (C), bovine (D) and equine (E) native oviductal tissue.

i) Gross anatomical features of oviductal fimbriae including the ovary in feline, canine, and porcine images (black circle).

The fimbriae of the infundibulum branches to tightly engulf the ovary (white arrow) in feline and canine. In the porcine, bovine and equine, the fimbriae projections are not adhered to the ovary but freely interact with the ovarian structure.

ii) Histological staining with H&E details the infundibular epithelium, lined with a single layer of polarised columnar epithelial cells. In each species, a highly folded mucosa with crypts is evident.

iii) Immunofluorescence imaging showing a consistent expression of PAX8 (red) positive secretory epithelial cells, located mostly along the basal region of the epithelial cells. Additionally, Ac-tubulin (green) is depicted staining the flagella-like projections of the epithelial ciliated cells. In the cat and dog Ac-tubulin positive ciliated cells were more irregularly spaced, compared to that in porcine, bovine, and equine. DAPI (blue) staining shows the nuclei of cells.

iii) Immunostaining depicting positive staining for Ki67 (red), strictly associated with cell proliferation constitutively. Cells can be seen dispersed throughout normal healthy oviductal epithelium. Additionally, mature ciliated cells are stained positive for Ac-tubulin (green) and cell nuclei are stained with DAPI (blue).

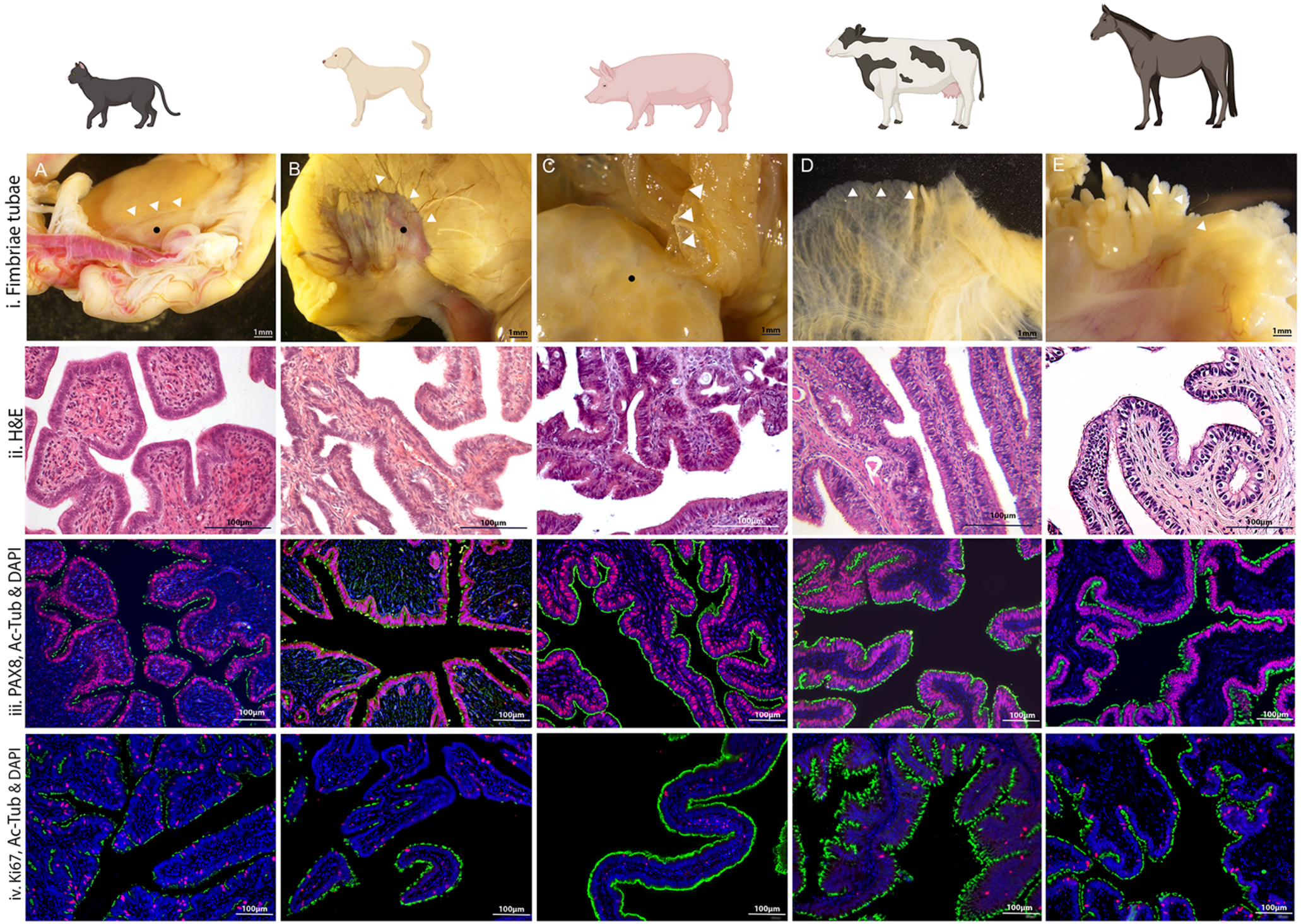
i. Fimbriae tubae
ii. H&E
iii. PAX8, Ac-Tub & DAPI
iv. Ki67, Ac-Tub & DAPI
A
B
C
D
E
1mm
100µm

Figure 2. Representative bright-field microscopy images showing organoid development from feline (A), canine (B), porcine (C), bovine (D) and equine (E) oviductal epithelial cells at Days 1, 6, 12, 18 and 21 of culture (I, ii, iii, iv and v, respectively). Maximal
individual organoid expansion can be observed occurring between Days 12 and 18. The scale bars shown on all images correspond to a length of 500 μm.

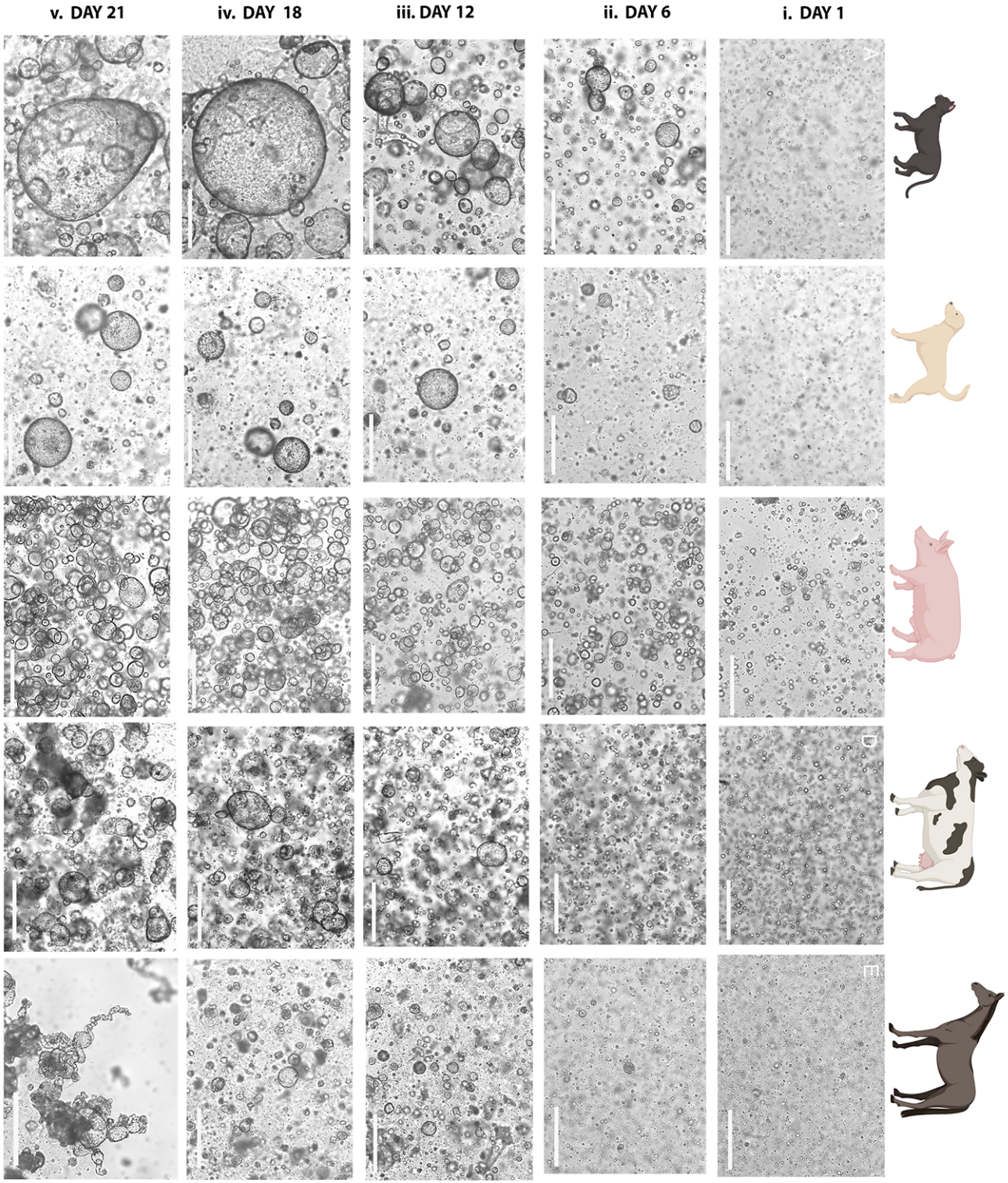
v. DAY 21
iv. DAY 18
iii. DAY 12
ii. DAY 6
i. DAY 1
A
B
C
D
E

Figure 3. High magnification (x20) brightfield images of feline (A) and equine (B) mature organoids at 21-days of culture. The equine organoids started branching as they matured and depicted a more varying and complex shape compared to the feline oviductal epithelial organoids, which remained more spheroid in structure. The scale bars correspond to a length of 125 μm.

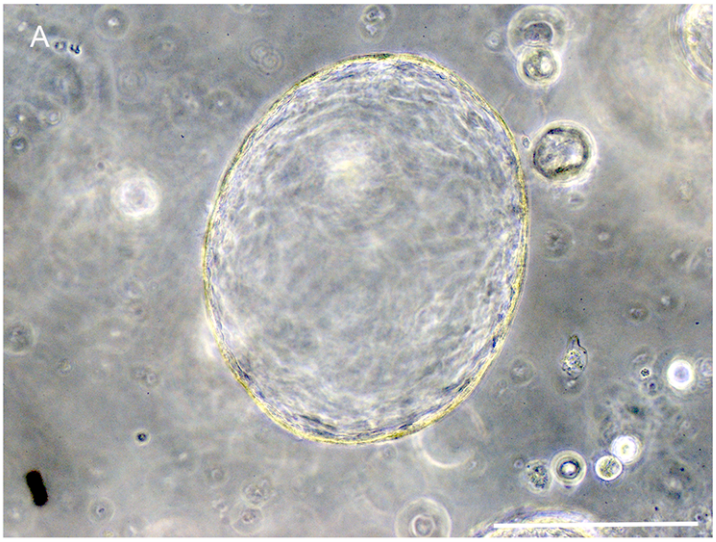
A

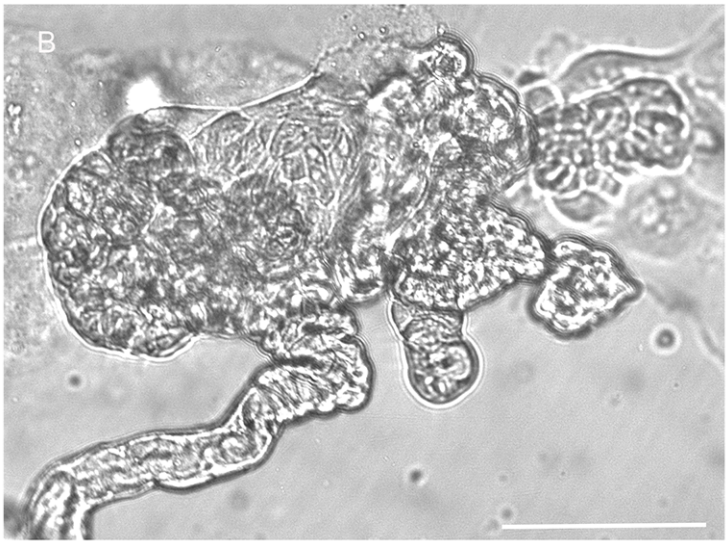
B

Figure 4. Characterisation of feline (A), canine (B), porcine (C), bovine (D) and equine (E) oviductal epithelial organoids at 21 days of culture.

i) Histological staining with H&E showing oviductal epithelial organoids with a monolayer of polarised columnar epithelial cells lining the lumen. In each species, a clear lumen is evident characterised by the presence of luminal crypts and folds.

ii) Immunostaining with PAX8 (red), Ac-Tubulin (green), and DAPI (blue) within epithelial cells. Positive staining for α-tubulin indicates ciliated cell differentiation. Positive PAX8 nuclear staining indicates the presence of progenitor secretory cells, which are non-ciliated. DAPI effectively stained the nuclei. Staining patterns mimicked that represented in native oviduct tissue.

iii) Positive identification of the marker for proliferating cells, Ki67 (red), showed it was constitutively dispersed and basally located throughout. Positive nuclear staining for Ki67 suggests that the cells were actively dividing. In addition, Ac-Tubulin (green) stained ciliated cells were identified together with the DAPI (blue) stained nuclei of cells. The scale bars shown on all images correspond to a length of 100 μm.

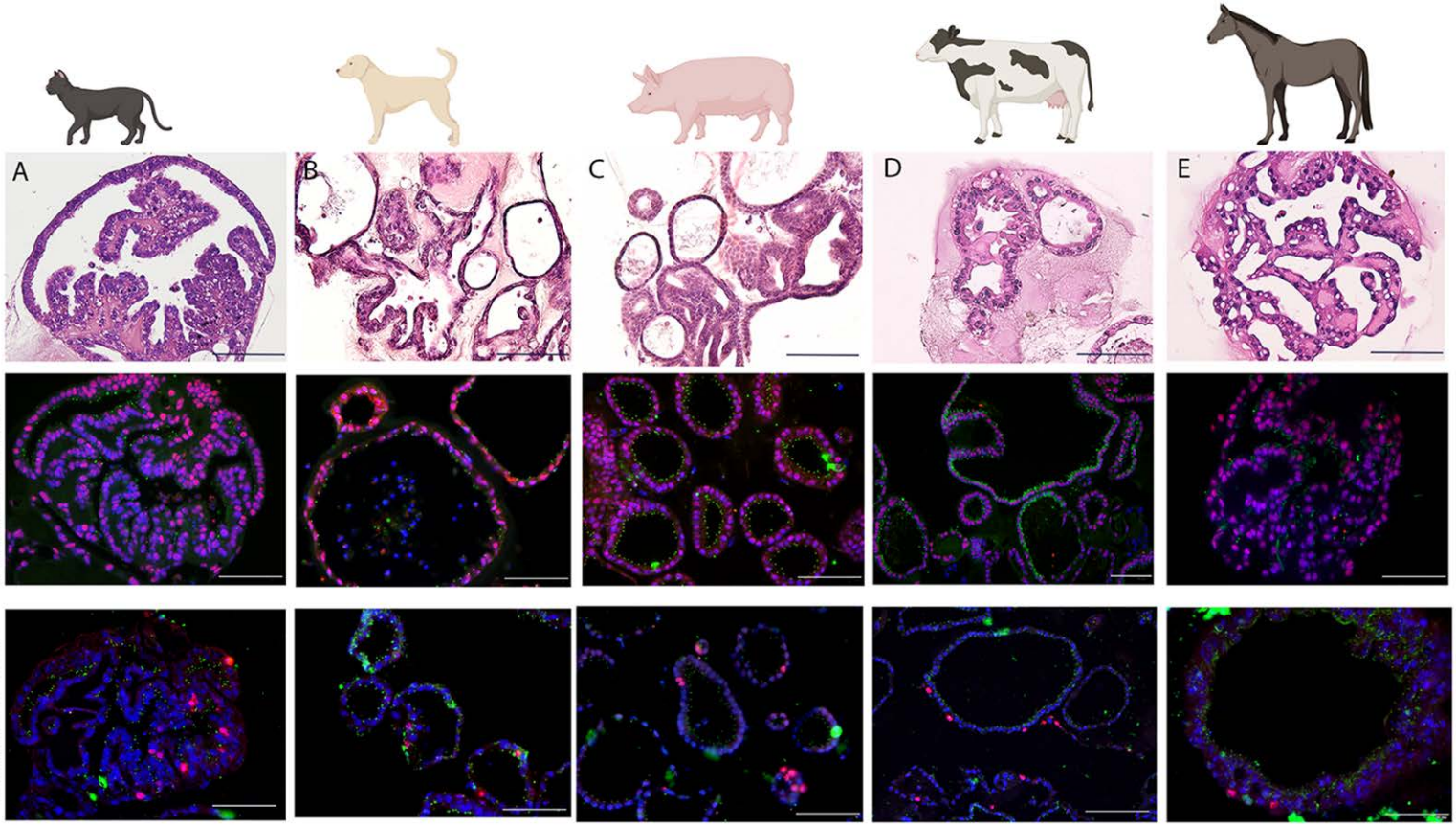
A
B
C
D
E
i. H&E
ii. PAX8, Ac-Tub & DAPI
iii. Ki67, Ac-Tub & DAPI

Figure 5. Representative immunofluorescent confocal images showing detailed cilia structures of porcine organoids at 21-days of culture. Ciliated cells contained abundant well-defined cilia, predominantly apically pointed, and anchored to well-aligned basal bodies. Those cells with acetylated microtubules showed positive staining (green) with Ac-Tubulin but were negative for PAX8 secretory cells and vice versa (A). In some of these cells, Ac-Tubulin positive cilia can be observed projecting into a different confocal plane of view (B). The scale bars correspond to a length of 4 μm.

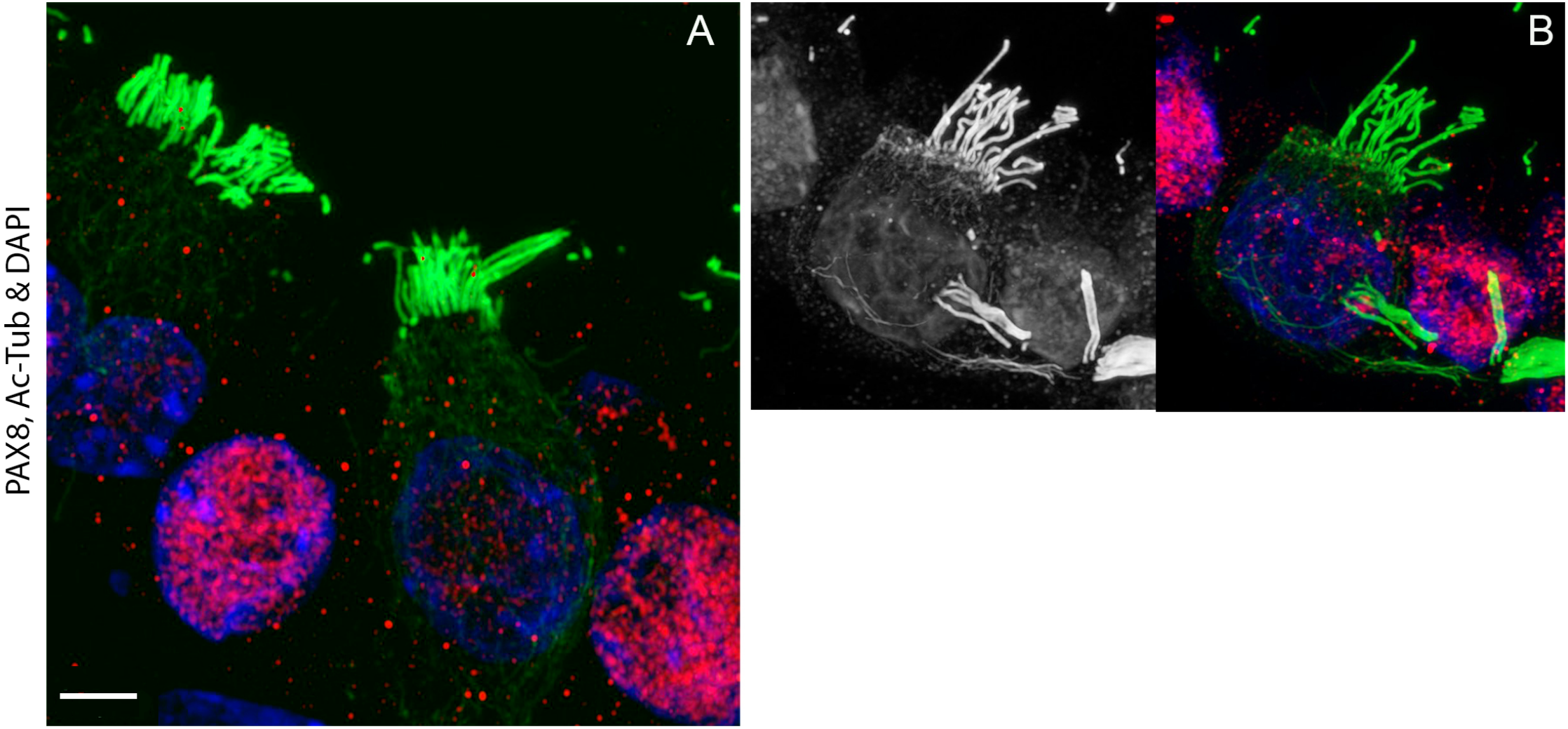
PAX8, Ac-Tub & DAPI
A
B

Figure 6. Quantification of organoid development from feline, canine, porcine, bovine and equine oviductal epithelial cells, over a period of 21 days in culture.

a) Quantification of the average area (μm^2) organoid size between species, at 1, 6, 12, 18 and 21 days of culture.

b) Each species represented via complexity index. Perimeter to area ratios measure the complexity of the 2D biological shape between organoid species. The higher the value the more complex the shape via the application of morphometrics.

c) Quantification and comparison of organoid sizes for each species, with area growth per day.

d) The distribution of organoid sizes over 21 days of culture according to area (μm^2).

a.

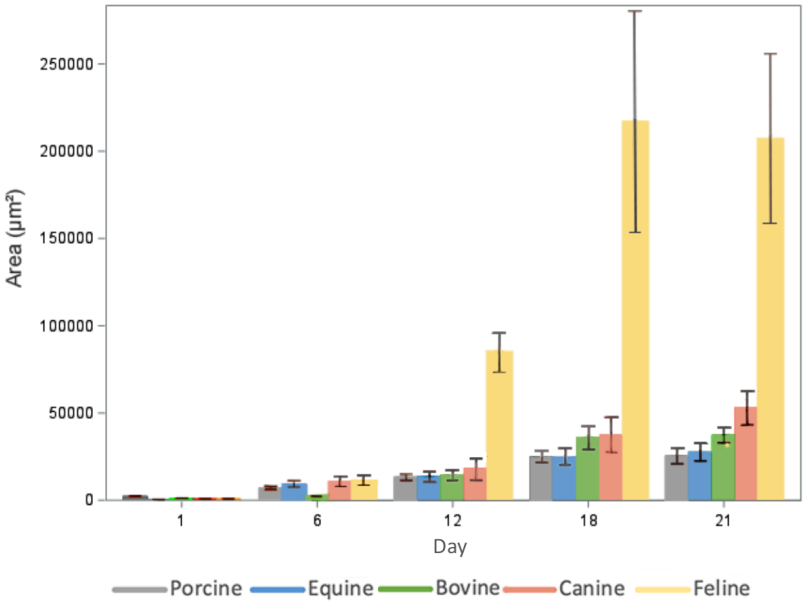
Area (µm²)
250000
200000
150000
100000
50000
0
1
6
12
18
21
Day
Porcine
Equine
Bovine
Canine
Feline

b.

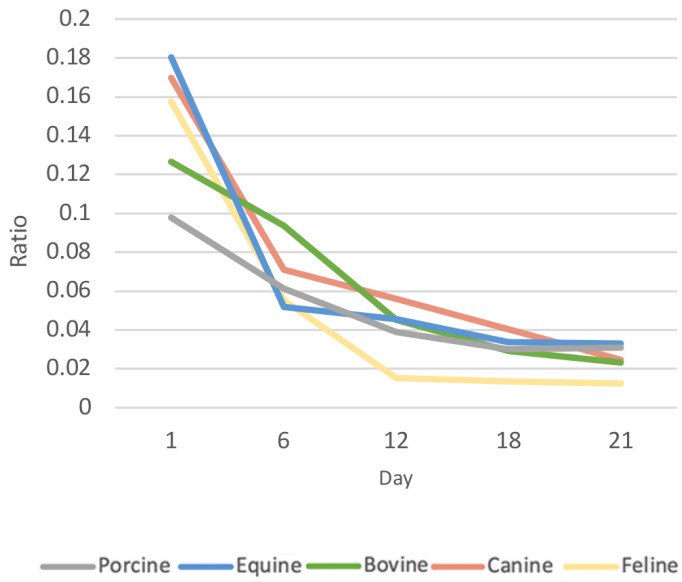
Ratio
0.2
0.18
0.16
0.14
0.12
0.1
0.08
0.06
0.04
0.02
0
1
6
12
18
21
Day
Porcine
Equine
Bovine
Canine
Feline

c.

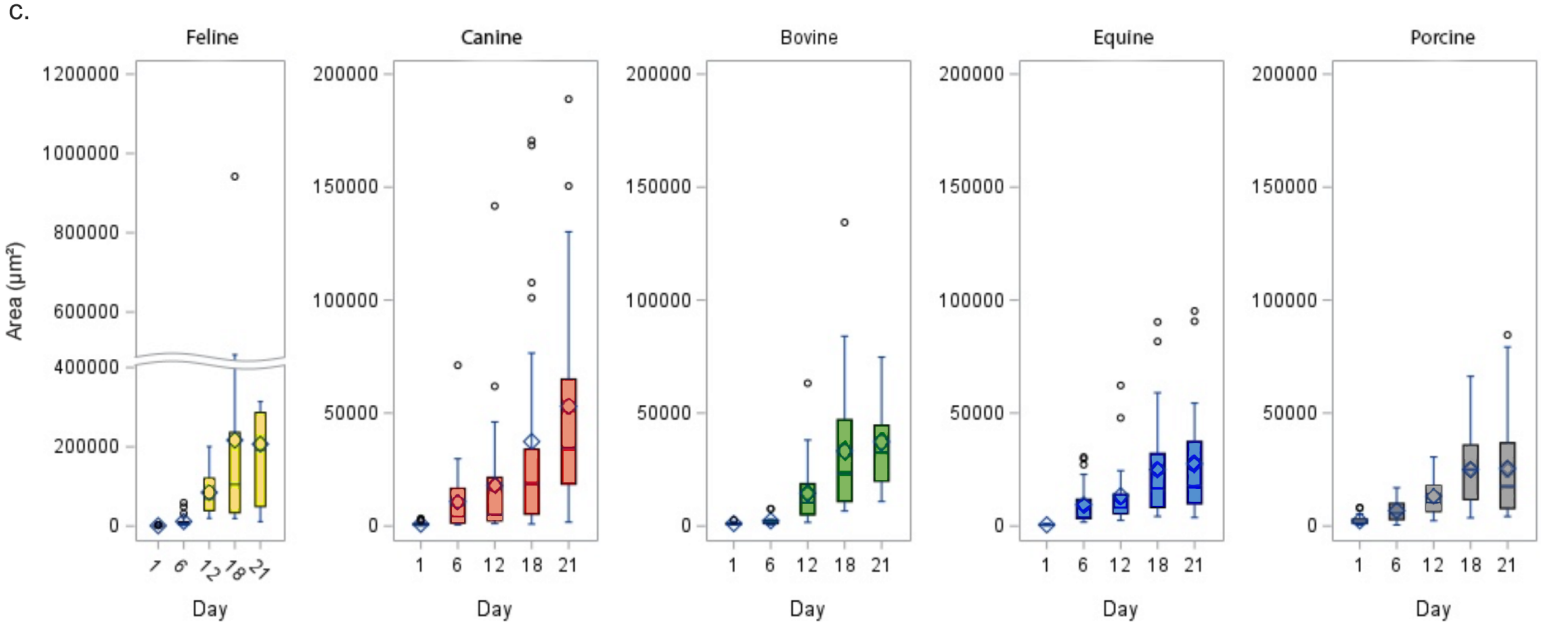
Feline
Canine
Bovine
Equine
Porcine
Area (µm²)
1200000
1000000
800000
600000
400000
200000
150000
100000
50000
0
1
6
12
18
21
Day

d.

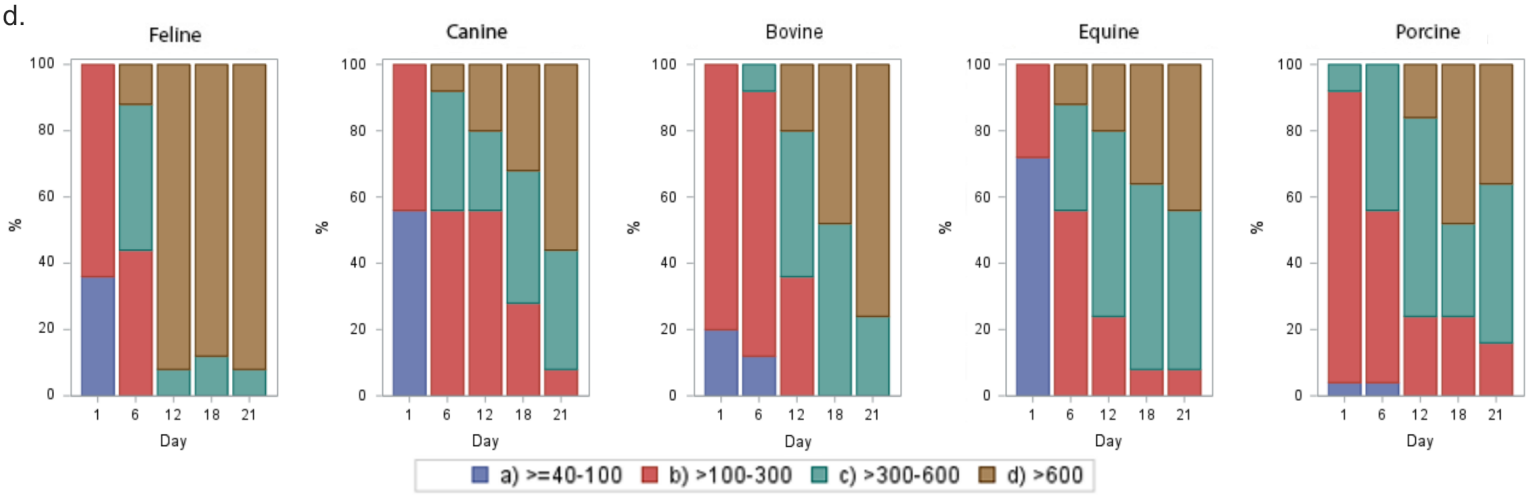
Feline
Canine
Bovine
Equine
Porcine
%
100
80
60
40
20
0
1
6
12
18
21
Day
a) >=40-100
b) >100-300
c) >300-600
d) >600